

Fig. 1. ^{57}Fe Mössbauer spectrum of Crater Elegante olivine at 295°K. The doublet results from Fe^{2+} at the M1 and M2 sites. The small peak at 0.7 mm/sec is assigned to the high velocity peak of a weak Fe^{3+} doublet. The low velocity peak of Fe^{3+} coincides with the low velocity peak of Fe^{2+} .

present while the olivine with no detectable Fe^{3+} has an activation energy of 1.2 eV.

3. Discussion

Fig. 2 is a plot of $\log \sigma_x$ vs mole % fayalite for all available σ data on olivine with activation energies A_x between 0.5 and 2.0 eV. Lower A_x are restricted to temperatures less than 500°C and seem to be related to an extrinsic semiconduction. Higher A_x are reported for temperatures greater than 1100°C and are variously described as due to ionic conduction or intrinsic semiconduction [6].

Using selected literature data and data they collected for olivines with 7.4, 8.4 and 12.6 mole% fayalite (Fa 7.4, etc.) Kobayashi and Maruyama [7] propose a relationship between $\log \sigma_x$ and mole % fayalite in olivine single crystals (line III in fig. 2) that implies an extremely high value of $\log \sigma_x$ for fayalite ($\log \sigma_x \cong 12$). If, on the other hand, all avail-

able literature data are plotted as in fig. 2, two interesting features appear:

- 1) The activation energies of all single crystal data below the line marked I are 1.0 eV or less, while above that line the activation energies are all greater than 1.0 eV.
- 2) The activation energies for all olivine powders below the line marked II are less than 1.0 eV and those above the line are greater than 1.0 eV.

For the olivines represented in fig. 2, numbers 3, 23, and 25b, c and e have $\text{Fe}_2\text{O}_3 > 0.05$ wt%; numbers 6, 7, 21, 25d and 27 have $\text{Fe}_2\text{O}_3 \leq 0.05$ wt%, and the Fe_2O_3 concentration of the others is not reported. Single crystal data in this group plot above line I for $\text{Fe}_2\text{O}_3 < 0.05$ wt% and below line I for $\text{Fe}_2\text{O}_3 > 0.05$ wt%. The powders behave similarly with respect to line II with the exception of number 7 (0.04 wt% Fe_2O_3); however, number 6 from this locality does plot above line 2. Perhaps experimental difficulties can account for this discrepancy.

The apparent "saturation" effect in $\log \sigma_x$ as a function of fayalite content along curve II for powders may be fortuitous as point 3 provides only a lower bound at 100% fayalite. Another possibility is that most of the experiments have been performed on olivines which have been oxidized in comparable fashion in the laboratory during synthesis [3, 4]. Because of the poor statistics and experimental uncertainties, no strong argument can be made for the locus of curves I and II. However, the grouping of the data indicated by these two lines is sufficient to imply that some property other than fayalite content has a controlling influence on conductivity in olivine in the temperature range from 500 to 1100°C.

Oxidation of the San Carlos olivine [6] during σ measurements resulted in an increased σ_x with no change in A_x [5, 6]. From this information alone, one could postulate that the A_x for electronic semiconduction in this temperature range, proposed by Bradley et al. [9] and supported by Hall effect measurements [10], is 0.7 eV. However, the range in A_x for olivines below lines I and II is from 0.5 eV to 1.0 eV. This large variation in activation energy may be related to Fe^{3+} concentration [7], other impurities, or even dislocation density variations among olivines [11].

From the relationships observed in fig. 2, it is proposed that the conductivity of olivine below

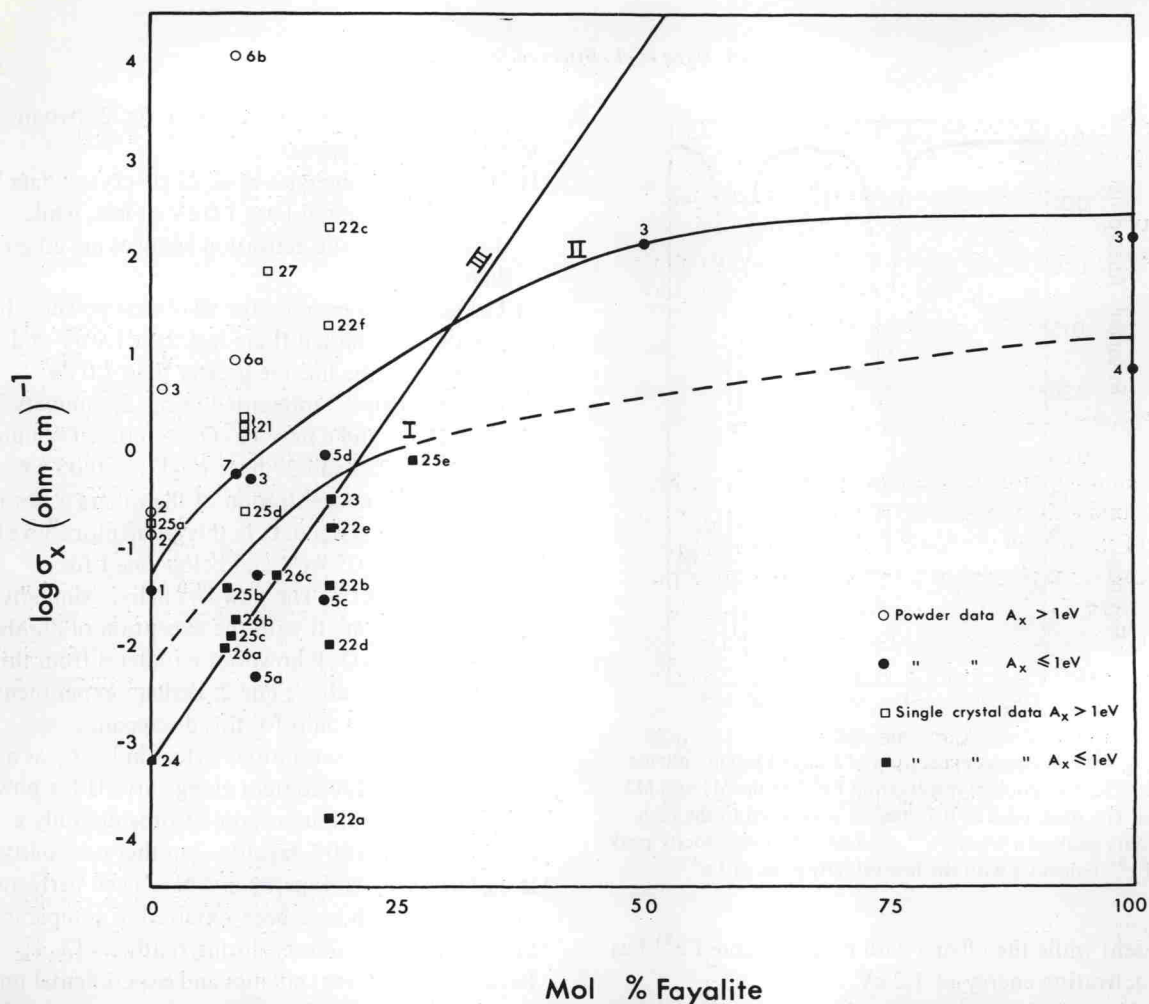


Fig. 2. $\log \sigma_x$ vs mol % fayalite for olivine powders and single crystals. Numbers beside the data points refer to studies indicated below:

Powders

1. Jander and Stamm [12]. Synthetic forsterite powder, 850–1200°C, $A_x = 0.92$ eV.
2. Hughes [4]. 2 synthetic forsterite powders. Below 900°C A_x was 1.02 and 1.43 eV. Above 900°C A_x was 3.1 and 3.3 with $\log \sigma_x = 7$ (not graphed).
3. Bradley et al. [9]. Synthetic olivine powders, 200–700°C, A_x ranges from 1.05 eV for 1% fayalite to 0.64 eV for 100% fayalite.
4. Akimoto and Fujisawa [13]. Synthetic fayalite, 31 kb, 150–900°C, $A_x = 0.51$ eV.
5. Hamilton [14]. Powders prepared from natural olivines, data plotted for 11.5 kb.
 - a) 250–450°C, 0.75 eV; b) 450–600°C, 0.91 eV; c) 250–325°C, 0.70 eV; d) 350–550°C, 0.90 eV.
6. Schult and Schober [15]. Natural olivine powder from Dreiser Weiher, Germany, 6 kb.
 - a) 250–600°C, $A_x = 1.28$ eV; b) 600–950°C, $A_x = 1.89$ eV.
7. Schober [10]. Natural olivine powder from Dreiser Weiher, Germany, 20 kb, $A_x = 0.70$ eV.

Single crystals

21. Hughes [4]. St. John's Island, Red Sea, Egypt, 700–1100°C, 3 sections, perpendicular and parallel to (010), A_x from 1.56 to 1.68 eV.
22. Noritomi [7]. Compositions not reported, assumed 18% fayalite by Mizutani and Kanamori [16]. Data \perp to (001) for Bonin Island not plotted since they do not differ much from (001) data which are plotted.
 - a) Sado, Japan, 300–450°C, 0.66 eV; b) Sado, Japan 450–600°C, 1.00 eV; c) Sado, Japan, 600–1050°C, 1.64 eV; d) Bonin Island, 300–500°C, 0.64 eV; e) Bonin Island, 500–625°C, 0.80 eV; f) Bonin Island, 625–1050°C, 1.25 eV.
23. Mizutani and Kanamori [16]. Miyake-jima olivine, $A_x = 0.86$ eV.
24. Shankland [17]. Synthetic forsterite with 0.2 mole% fayalite, $A_x = 1.00$ eV.
25. Duba [5]. 7.5 kb.
 - a) Synthetic forsterite, 700–1100°C, 1.70 eV.
 - b) Mt. Leura, Camperdown, Victoria, Australia, 250–700°C, 0.85 eV.
 - c) San Carlos Indian Reservation, Arizona, U.S.A., 150–700°C, 0.69 eV, (001). (010) and (100) data do not differ significantly and are not plotted to avoid excessive crowding.
 - d) St. Johns's Island, Red Sea, Egypt, 500–1100°C, 1.21 eV, (010).
 - e) Crater Elegante, Sonora, Mexico, 200–700°C, 0.76 eV.
26. Kobayashi and Maruyama [7]. Data were collected for the 3 principal directions for each of the olivines below. Since σ differs only slightly with crystallographic orientation, only one determination for each composition is plotted.
 - a) Buhell Park, Arizona, U.S.A., 500–950°C, 0.80 eV (100).
 - b) Buhell Park, Arizona, U.S.A., 450–950°C, 0.79 eV (100).
 - c) Karatsu, Japan, 500–950°C, 0.81 eV (010).
27. Schober [10]. Brazil, 20 kb, 600–1300°C, $A_x = 1.09$ eV.